AIAA 80-0457R

A Method for Measuring the Stability of a Full-Scale Rotor Control System

Inderjit Chopra* and John Ballard†
NASA Ames Research Center, Moffett Field, Calif.

In the development of rotor systems that use active feedback to augment the dynamic control characteristics of the aircraft, a safe and efficient method of testing the control system is required. A stoppable rotor with blade circulation blowing was tested in the Ames 40×80 ft wind tunnel. A major part of the test schedule was dedicated to the acquisition of data to determine the stability of a closed-loop hub-moment feedback control system. The open-loop control response was measured at several flight conditions to ascertain the stability of the system prior to final closed-loop feedback control testing. Measurements were made during both stopped and rotating modes of rotor operation, and Bode plots were obtained for the control loops associated with the moments about the longitudinal and lateral axes.

Introduction

A MAJOR milestone in any aircraft design and development is the demonstration of satisfactory dynamic flight characteristics. The determination of these flight characteristics forms a significant part of the wind-tunnel test programs for these aircraft. This paper describes a method for the measurement and calculation of the stability of an aircraft feedback control system using a frequency-response method, and documents its successful application with a full-scale rotor system.

A stoppable rotor model with a hub-moment feedback control system was tested in the NASA Ames 40×80 ft wind tunnel, and stability measurements were made in both fixed and rotary wing modes. The open-loop control testing for the pitch-moment and roll-moment feedback was done over a range of operating conditions. The data acquisition and analysis was accomplished online using a minicomputer-based time-series analysis system. The command actuators for the pitch and roll modes were excited by a banded white noise signal and a transfer function of the response was determined. Bode plots of the averaged transfer function were used to obtain the stability margins.

Feedback Control System

The closed-loop transfer function of a ›nventional feedback control system is

$$\frac{Y(s)}{X(s)} = \frac{G(s)}{1+G(s)H(s)}$$

where $X(s)$ is the Laplace transform of the control input, $Y(s)$ the system response, $G(s)$ the forward-path transfer function, and $H(s)$ the transfer function of the feedback path. The product $G(s)H(s)$ is the open-loop transfer function. The stability of a closed-loop system can be determined from the frequency response of the open-loop system.[1]

A simplified block diagram of the feedback control system analyzed in this paper is shown in Fig. 1; a photograph of the stoppable rotor is shown in Fig. 2. The faired body module contained four load cells attached to the rotor hub and supporting structure. These load cells were used as the pitch and roll moment sensors (Fig. 1). Circulation control was provided by airflow ducted to spanwise leading- and trailing-edge slots on the four blades. Thus, the lift was controlled by blowing (Coanda Principle) and was a function of the blowing momentum coefficient C_μ, where

Rotary wing mode:

$$C_\mu = \frac{\dot{m}V_j}{\frac{1}{2}\rho(\Omega R)^2 c}$$

Fixed wing mode:

$$C_\mu = \frac{\dot{m}V_j}{\frac{1}{2}\rho V^2 c}$$

where $\dot{m}V_j$ is jet momentum flux per length, ρ is air density, V is wind-tunnel airspeed, c is the blade chord, and ΩR is the rotor tip speed. The pitch and roll control servos regulated pneumatic actuators which varied the circulation blowing over the blade surfaces on a cyclic (once per revolution) schedule. The open-loop hub-moment feedback control measurements were obtained by breaking the forward path circuit after the first amplifier. The input signal was applied to the integrator, while the associated response signal was measured at the output of the amplifier. For the closed-loop hub-moment feedback control system operation, the signals from the hub-moment sensors were conditioned by a series of low-pass filters and an integrator to obtain a proper closed-loop response.

Data Acquisition and Analysis

A schematic of the test arrangement and data reduction is shown in Fig. 3. The signal from the random signal generator was passed through a bandpass filter to obtain the banded white noise. The magnitude of the input signal to the model actuator was adjusted with a potentiometer. The input and response signals were monitored on an oscilloscope. The amplitude of the input signal was selected after considering various factors such as signal/noise ratio, actuator limits, and the possibility of overstressing the model.

The online data reduction for the single-input, single-output transfer function was made using a minicomputer-based time-series analysis system. When the model was being

Presented as Paper 80-0457 at the AIAA 11th Aerodynamic Testing Conference, Colorado Springs, Colo., March 18-20, 1980; submitted March 23, 1980; revision received Aug. 14, 1980.

*Senior Research Associate, NASA/Stanford Joint Institute for Aeronautics and Acoustics, Stanford, Calif. Member AIAA.

†Research Scientist. Member AIAA.

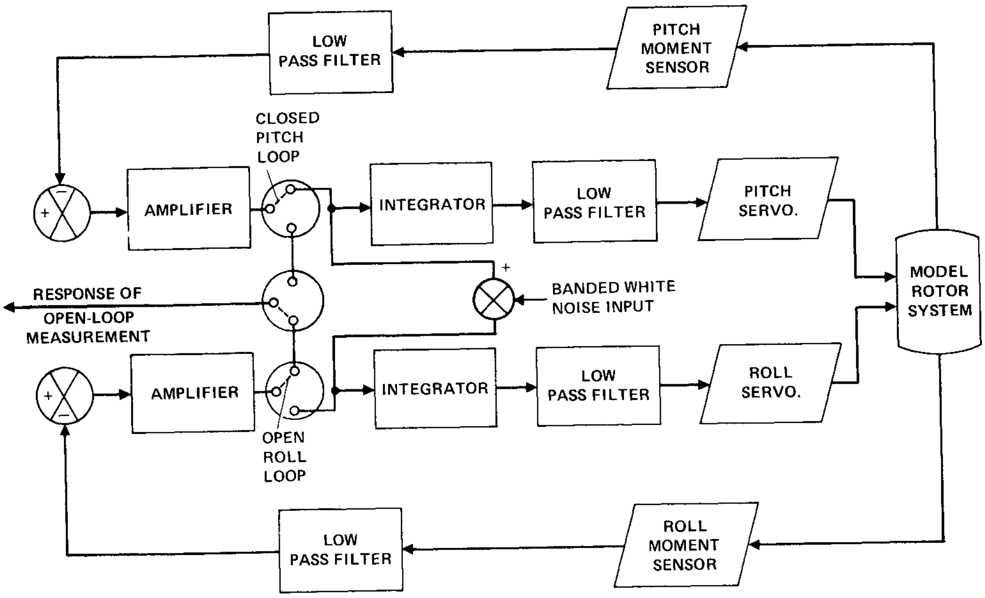

Fig. 1 Simplified block diagram of the rotor model with hub-moment feedback control system during open-loop testing.

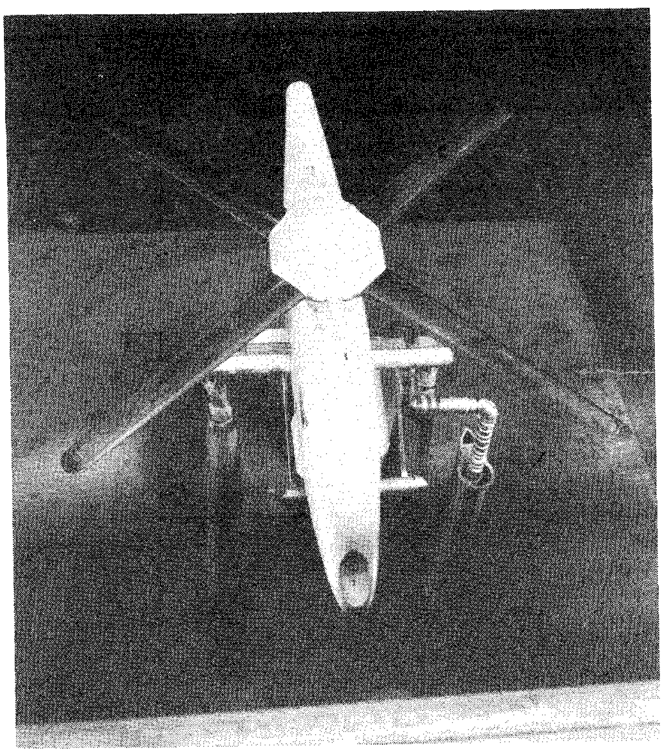

Fig. 2 Photograph of rotor model in NASA Ames Research Center 40 × 80 ft wind tunnel.

excited, the input signal and the response signal were sampled and digitized at a rate of r (per second). After N samples of data were obtained, the discrete Fourier transform of the data set was made. The cross-spectrum of the input and output transforms and the autospectrum of the input transforms were then calculated as follows:

$$S_{yx} = Y^* \bar{X} \qquad S_{xx} = X^* \bar{X}$$

where $\bar{X}$ is the complex conjugate of X. As shown in Fig. 3, the data acquisition, Fourier transform, and spectra calculation were repeated K times. After the final (Kth) spectra was obtained, the input excitation to the model actuator was removed. The transfer function was calculated from the ratio of the averaged values of cross-spectrum and the averaged autospectrum.

The dynamic response is presented in Bode plots. A Bode plot consists of two graphs, the magnitude (in dB) and the phase angle (in deg) of the complex transfer function H plotted as function of frequency:

$$\text{Magnitude} = 20 \log |H|, \text{ dB}$$

$$\text{Phase} = 57.3 \tan \angle H, \text{ deg}$$

From these plots, gain margin and phase margin may be obtained which define the relative stability of the control loop under examination. Gain margin is defined as the magnitude of the transfer function (in dB) evaluated at the frequency where the phase angle is −180 deg (see Fig. 4a). The gain margin shows the additional gain needed to render the system marginally unstable.

The governing critical parameters for the transfer function measurements were the sample rate r, the number of samples N in a set, the number of averages K, and the frequency range of white noise. The discrete Fourier transform results in a total of $N/2$ complex numbers, with a maximum frequency of $r/2$ Hz (Nyquist frequency). The sample rate r was at least 2.5 times the maximum frequency of interest to avoid aliasing. The time period T for recording a single data set was N/r and, therefore, the frequency resolution was r/N (i.e., $1/T$). The total time to acquire K averages of the recorded data sets was KT seconds. The choice of the total number of samples N was determined from the desired frequency resolution and the total test time available. By increasing the number of records K, a reduction in the background noise level was possible. Therefore, increasing the number of records reduces the error level, but it also increases the total sample time. The break frequency at the bandpass filter was chosen so that the input energy was concentrated in the frequency range of interest and alias error was avoided. Additional discussion of parameter selection and parameter compromises may be found in Ref. 2.

The following parameters were selected for the data acquisition:

Sample rate, r	= 51.2 Hz
Number of samples, N	= 256
Frequency resolution	= 0.2 Hz
Number of averages, K	= 20
Total sample time	= 100 s
Bandpass filter range	= 1-15 Hz

Wind Tunnel Test Results

Figure 2 shows the model in the 40 × 80 ft wind tunnel. The model was a stoppable rotor which operated in fixed-wing as

Table 1 Hub-moment feedback control loop condition

Fig.	Rotor operation	Roll loop	Pitch loop	C_μ
4a	Rotary wing	Stability test	Open-loop	0.0068
4b	Rotary wing	Open-loop	Stability test	0.0068
4c	Rotary wing	Stability test	Closed-loop	0.0068
4d	Rotary wing	Closed-loop	Stability test	0.0068
5a	Fixed wing	Stability test	Open-loop	0.0220
5b	Fixed wing	Open-loop	Stability test	0.0220
5c	Fixed wing	Stability test	Closed-loop	0.0220

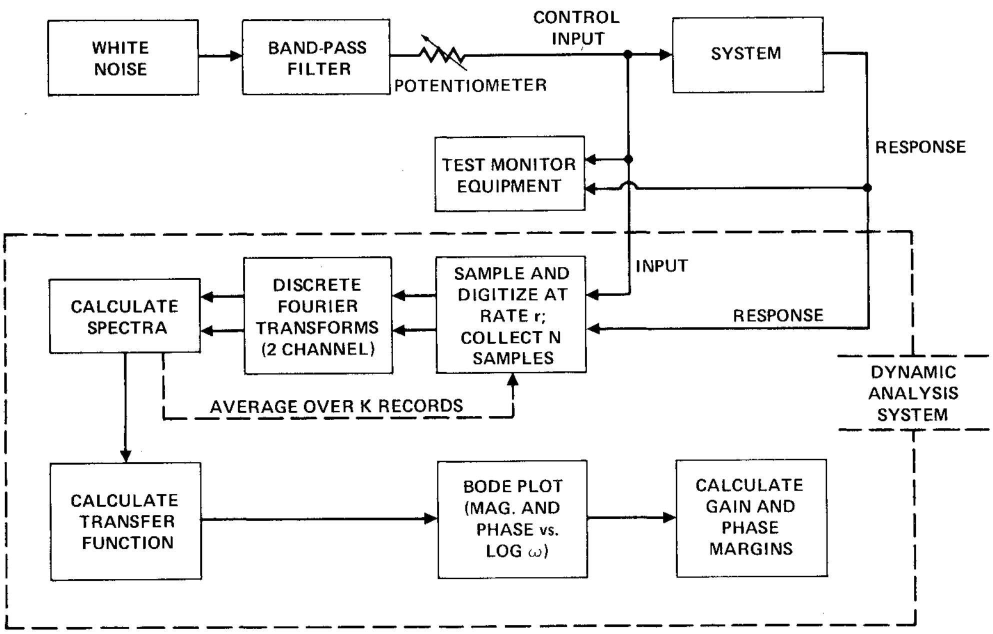

Fig. 3 Measurement system and transfer function algorithm.

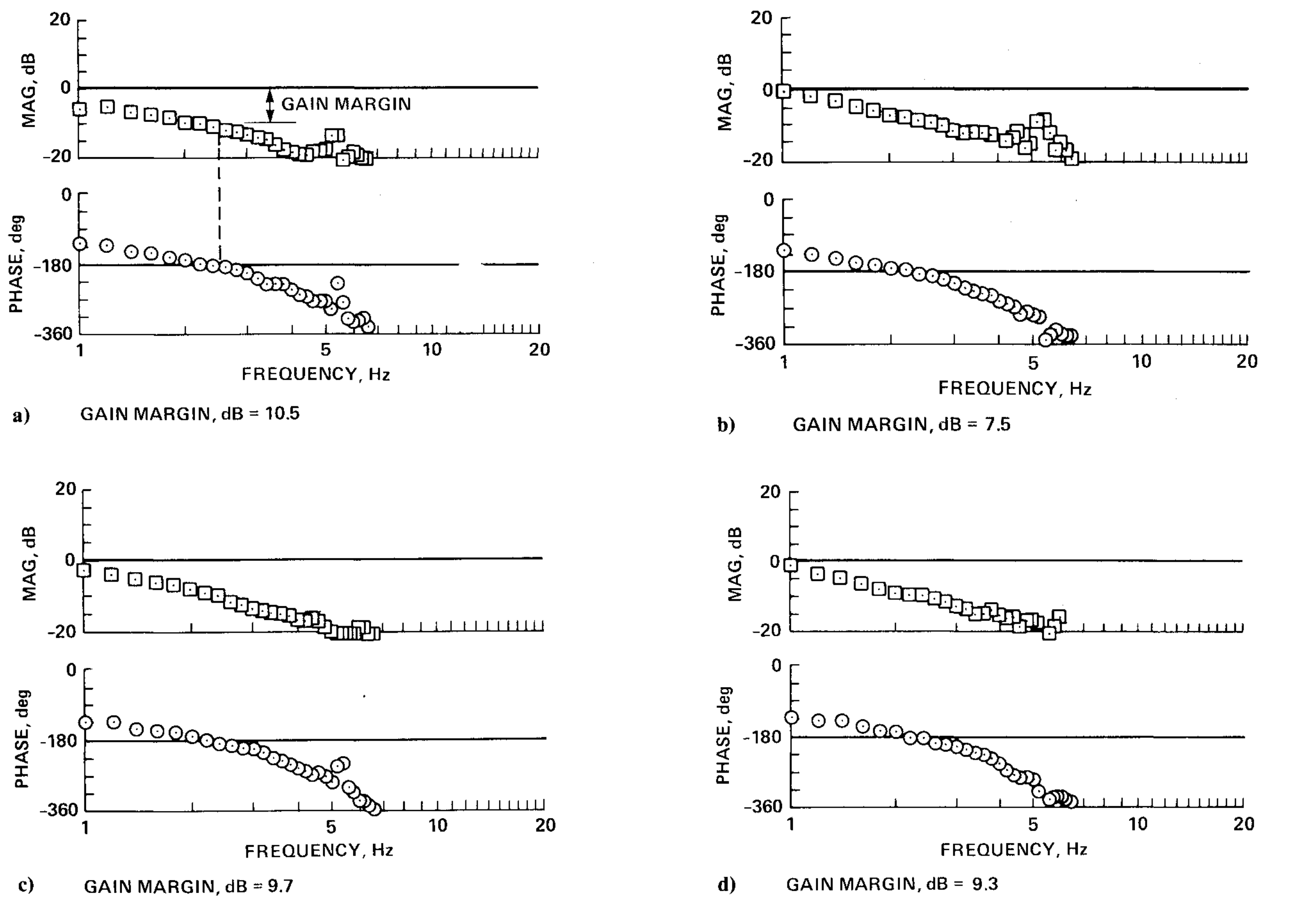

Fig. 4 Bode plot of measured hub-moment feedback control system stability, rotary wing mode: a) roll mode stability with pitch loop open; b) pitch mode stability with roll loop open; c) roll mode stability with pitch loop closed; d) pitch mode stability with roll loop closed.

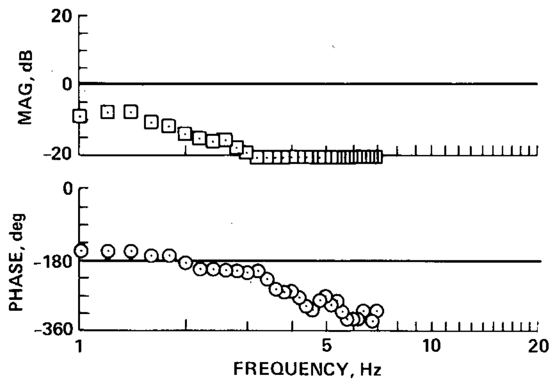

a) GAIN MARGIN, dB = 12.7

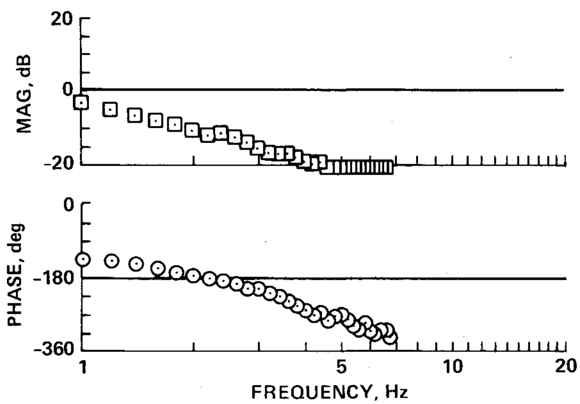

b) GAIN MARGIN, dB = 11.0

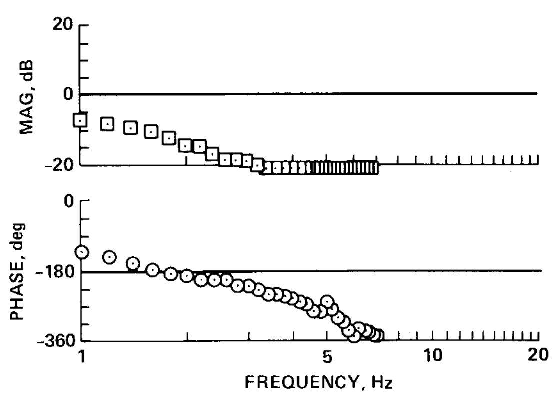

c) GAIN MARGIN, dB = 12.6

Fig. 5 Bode plot of measured hub-moment feedback control system stability, fixed wing mode: a) roll mode stability with pitch loop open; b) pitch mode stability with roll loop open; c) roll mode stability with pitch loop closed.

well as rotary-wing modes. The open-loop stability measurements were made over a range of tunnel operating conditions and model rotational speeds in both the roll and pitch modes. Figures 4 and 5 present typical results of the stability measurements, in Bode plot format, for the rotary- and fixed-wing modes, respectively. For both rotor modes, the operating conditions were as follows:

Tunnel freestream velocity, V	= 92 m/s
Rotor disk angle of attack	= 2 deg
Rotor blade pitch angle at 0.75 R	= −4 deg

The rotor rotational speed for the rotary wing mode was 33.5 rad/s. The rotor and control system configuration for the cases shown in Figs. 4 and 5 are summarized in Table 1.

Control system stability can be compared through the gain margin parameter. The larger the gain margin magnitude, the more stable the system. Thus, comparison of Figs. 4a and 4b indicates that the roll mode is more stable than the pitch mode. Figure 4c, when related to Fig. 4a, shows that the roll mode is insensitive to the closing of the pitch loop. Figure 4d, when viewed with respect to Fig. 4b, indicates that the pitch mode becomes more stable when the roll loop is closed. Similar results can be seen in a comparison of Figs. 5a-c for the fixed-wing mode, with the exception of increased pitch mode stability when the roll loop is closed. Due to other test considerations for the fixed-wing mode, pitch-mode testing with the roll loop closed was not performed. It should be noted that the blowing momentum coefficient was increased for the fixed wing case (the system overall loop gain is proportional to the blowing momentum coefficient). An expanded set of results can be found in Ref. 3.

Conclusions

A stoppable rotor with blade circulation blowing was tested in the NASA Ames 40 × 80 ft wind tunnel. During the test, the open-loop control response was measured at several flight conditions to determine the stability of the closed-loop, hub-moment feedback control system. The open-loop Bode plots indicate that the rotor has very good stability characteristics. This was proven by the successful completion of closed-loop testing of the rotor in the wind tunnel.

The test technique outlined in this paper allows rapid acquisition of high-quality stability data. The data reduction and analysis process was accelerated efficiently through the use of an online minicomputer-based time-series analysis system. Throughout this procedure, safety criteria were easily met by the initial testing of open-loop responses before proceeding to the closed-loop hub-moment feedback control system testing.

References

[1] D'Azzo, J.J. and Houpis, C.H., *Feedback Control System Analysis and Synthesis,* 2nd ed., McGraw-Hill Book Co., New York, 1966.

[2] Johnson, W., "Development of a Transfer Function Method for Dynamic Stability Measurement," NASA TN D-8522, 1977.

[3] Ballard, J., McCloud, J., and Forsyth, T., "An Investigation of a Stoppable Helicopter Rotor with Circulation Control," NASA TM X-81218, 1980.